ICAS-88-5.2.1

DELAMINATION BUCKLING OF CYLINDRICAL LAMINATES

G. J. Simitses*, Z. Q. Chen** and S. Sallam***
Georgia Institute of Technology, Atlanta, Georgia

Abstract

Models for predicting delamination buckling of laminated complete thin cylindrical shells and cylindrical panels are developed. The load cases are uniform axial compression and uniform pressure, applied individually. The models are different for the two load cases and by design they are kept as simple as possible. This is done in order to keep the mathematical representation of the model and the associated solution simple enough to permit extensive parametric studies. Through these studies one can identify important structural parameters and fully assess their effect on the critical load. Among the general conclusions one may list that (a) the most influencing parameters for a given laminated geometry is the size of the delamination, and its through-the-thickness position for both load cases, and (b) the effect of boundary conditions (along the straight edges) has an important effect for the case of pressure. On the other hand, for axial compression the effect of boundary conditions (ends) is insignificant for large delaminations.

I. Introduction

Cylindrical shells and panels are widely used as primary structures in several applications. These are often subjected to destabilizing loads. Therefore, buckling is an important failure mode and it forms a fundamental consideration in the design of such systems.

The advent of fiber reinforced composite materials has resulted in a significant increase of their use as a construction material, because of their many advantages, especially their high potential weight and overall cost savings. It was necessary then to investigate the buckling characteristics of laminated cylindrical shells. Initially, the studies were confined to configurations, which are free of defects, such as delaminations.

Composite structures often contain delaminations. Causes of delamination are many and include tool drops, bird strikes, runway debris hits, and manufacturing defects. The presence of delamination in a composite material may cause local buckling and therefore a reduction in the overall stiffness of the structure. The problem of delamination buckling has received attention in recent years.

A finite element analysis was developed by Whitcomb [1] to analyze a laminated plate with a through-the-width delamination. The postbuckling behavior was studied. In the parametric study, stress distributions and strain-energy release rates were calculated for various delamination lengths, delamination depths, applied loads, and lateral deflections. Some delamination growth data were obtained through fatigue tests. Another paper in this subject was presented by the above author and Shivakumar [2], in 1985, in which the buckling of an elliptic delamination embedded near the surface of a thick quasi-isotropic laminate was studied. Both the Finite Element and the Rayleigh-Ritz methods were used for the analysis. The Rayleigh-Ritz method was found to be simple, inexpensive, and accurate, except for highly anisotropic delaminated regions. In that paper, effects of delamination shape and orientation, material anisotropy, and layup on buckling strains were examined.

Yin and Wang [3] derived a simple expression for the energy release rate associated with the growth of a general one-dimensional delamination. The energy release rate was evaluated by means of the path-independent J-integral. Yin and Fei [4] investigated the buckling characteristics of a circular plate with a near-surface concentric delamination.

Angle-ply composite sandwich beams with through-the-width delaminations were studied by Gillespie and Pipes [5]. Reduction in flexural strength was found to be directly proportional to the length of delamination and varied from 41% to 87% of the original value.

Wang [6] investigated the behavior of angle-ply composite laminates with edge delamination. Based on a recently developed theory of laminated anisotropic elasticity, the problem was formulated using Lekhnitskii's complex variable stress potentials. An eigenfunction expansion method was employed to solve the singular elasticity problem. With the aid of a boundary collocation technique, complete stress and displacement fields were obtained.

A two-dimensional analytical model was developed by Chai and Babcock [7] to assess the compressive strength of near-surface interlaminar defects in laminated composites. The postbuckling solution for the delaminated elliptic sections was obtained by using the Rayleigh-Ritz method, while an energy balance criterion based on a self-similar disbond growth governed fracture.

* Professor of Aerospace Engineering
** Postdoctoral Fellow
*** Currently with the Aerospace Corporation, El Segundo, CA

Simitses, Sallam and Yin [8-10] investigated delamination buckling and growth of flat composite structural elements. A simple one-dimensional model was developed to predict critical loads for delaminated plates with both simply supported and clamped ends. The effects of delamination position, size, and thickness on the critical loads were studied in detail. The postbuckling behavior as well as the energy release rate were examined. The results revealed that the damage tolerance of the laminate was either governed by buckling or by the fracture toughness of the material.

Almost all the papers about delamination buckling deal with beams and plates. Owing to its complexity in mathematics, very limited information on the subject of delamination buckling of shells is currently available.

Troshin [11] studied the effect of longitudinal delamination, in a laminar cylindrical shell, on the critical external pressure. The shell was assumed to be separated by the delamination into three panels. A system of eight ordinary differential equations were derived from the governing partial differential equations. The system along with boundary and continuity conditions was integrated by the Kutta-Merson method with intermediate orthonormalization of solution vectors. Critical pressures for various locations and sizes of the delamination were found. In another paper [12], the same author investigated the delamination stability of triple-layered shells with almost the same method.

This paper deals primarily with the question of delamination buckling of cylindrical shells and panels and how the presence of the delamination affects the global load carrying capacity of a laminated structure.

II. Description of Mathematical Models

Models for predicting delamination buckling of laminated, complete, thin cylindrical shells and cylindrical panels are developed (see Fig. 1). The load cases are uniform axial compression and uniform pressure, applied individually. It is assumed that under subcritical loads the delamination does not expand.

II.1. Axial Compression Case

In the axial compression case, the delamination extends along the entire circumference of the cylindrical shell, on a surface parallel to the reference surface (see Fig. 1a). The location and size of the delamination is arbitrary and the boundary conditions are either simply supported or clamped. Delamination separates the cylindrical shell into four regions (four thin-walled cylindrical shells), such that each region is symmetric with respect to its own mid-surface. Let u_i, v_i, w_i (i = 1, 2, 3, 4) be the displacement components of material points on the mid-plane of each region (each cylindrical shell) in the x, y and z directions, respectively.

In Fig. 1a, $\underline{a}$ denotes the size of the delamination, while $\underline{l}$ and $\underline{b}$ denote its location from the left and right ends, respectively.

The buckling equations are derived by employing a perturbation technique. Since the perturbed state can be chosen to be infinitesimally close to the primary state, only first order terms in the admissible variations are retained.

In terms of the in-plane and transverse small additional displacements $(u_i, v_i, w_i)(i=1,2,3,4)$, the buckling equations take the form

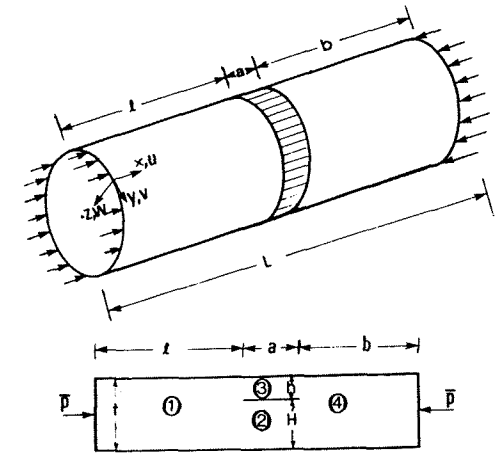

(a) Axial Compression

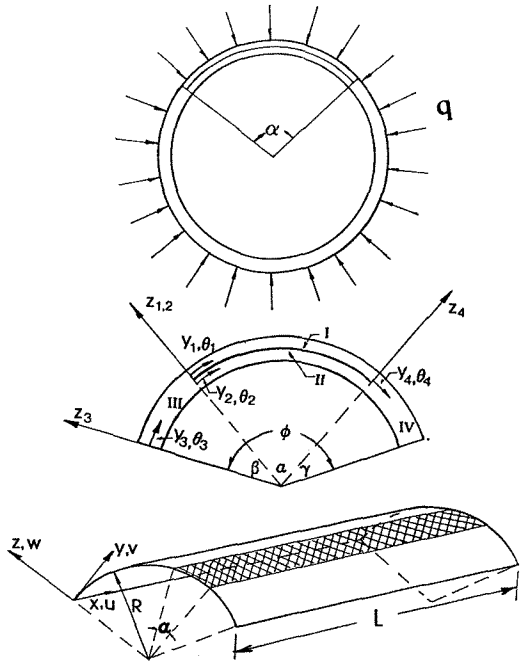

(b) Uniform Pressure

Fig. 1. Geometry, Loading any Sign Convention

$$D_{xx_i} w_{i,xxxx} + 2(D_{xy}+2D_{ss})_i \, w_{i,xxyy} + D_{yy_i} w_{i,yyyy} + \bar{N}_{xx_i} w_{i,xx} - \{ A_{xy_i} u_{i,x} + A_{yy_i} (v_{i,y} - w_i/R) \}/R = 0 \quad (1)$$

$$L_{1_i} u_i + L_{2_i} v_i = A_{xy_i} w_{i,x}/R \quad (2)$$

$$L_{2_i} u_i + L_{3_i} v_i = A_{yy_i} w_{i,y}/R \quad (3)$$

where the differential operators L_1, L_2 and L_3 are given by

$$L_1 = A_{xx} \, \partial^2 / \partial x^2 + A_{ss} \, \partial^2 / \partial y^2$$

$$L_2 = (A_{xy} + A_{ss}) \, \partial^2 / \partial x \partial y$$

$$L_3 = A_{ss} \, \partial^2 / \partial x^2 + A_{yy} \, \partial^2 / \partial y^2$$

and A_{ij}, D_{ij} (i,j = x,y,s) are the extensional and flexural stiffnesses. Note that in deriving the buckling equations, Donnell-type kinematic relations are employed.

The buckling equations are subject to auxiliary conditions. These conditions are grouped into three categories: Boundary Conditions, Kinematic Continuity Conditions, and Balance of Moments and Forces at the common boundaries.

Boundary Conditions:

Along each end of the cylindrical shell four boundary conditions have to be satisfied. For both simply supported and clamped boundaries, the following possibilities hold [13].

a) Simply Supported

SS1 $w_j = w_{j,xx} = N_{xx_j} = N_{xy_j} = 0$

SS2 $w_m = w_{j,xx} = u_j = N_{xy_j} = 0$ (4)

SS3 $w_j = w_{j,xx} = N_{xx_j} = v_j = 0$

SS4 $w_j = w_{j,xx} = u_j = v_j = 0$

b) Clamped Support

CC1 $w_j = w_{j,x} = N_{xx_j} = N_{xy_j} = 0$

CC2 $wi = w_{j,x} = u_j = N_{xy_j} = 0$ (5)

CC3 $w_j = w_{j,x} = N_{xx_j} = v_j = 0$

CC4 $w_j = w_{j,x} = u_j = v_j = 0$

where j = 1 at x = 0 and j = 4 at x = L, N_{xx}, N_{xy}, N_{yy} are small additional stress resultants needed to move from the primary state to the buckled one.

Kinematic Continuity Conditions

at x = l

$$u_1 - \frac{h}{2} w_{1,x} = u_2$$
$$u_2 + \frac{H}{2} w_{1,x} = u_3 \quad (6)$$

$$v_1 - \frac{h}{2} w_{1,y} = v_2$$
$$v_1 + \frac{H}{2} w_{1,y} = v_3 \quad (7)$$

$$w_1 = w_2 = w_3 \quad (8)$$

$$w_{1,x} = w_{2,x} = w_{3,x} \quad (9)$$

at x = l + a

$$u_4 - \frac{h}{2} w_{4,x} = u_2$$
$$u_4 + \frac{H}{2} w_{4,x} = u_3 \quad (10)$$

$$v_4 - \frac{h}{2} w_{4,y} = v_2$$
$$v_4 + \frac{H}{2} w_{4,y} = v_3 \quad (11)$$

$$w_4 = w_2 = w_3 \quad (12)$$

$$w_{4,x} = w_{2,x} = w_{3,x} \quad (13)$$

Balance of Moments and Forces

x = l

$$M_{xx_1} - M_{xx_2} - M_{xx_3} - N_{xx_2} \frac{h}{2} + N_{xx_3} \frac{H}{2} = 0 \quad (14)$$

$$N_{xx_1} - N_{xx_2} - N_{xx_3} = 0 \quad (15)$$

$$N_{xy_1} - N_{xy_2} - N_{xy_3} = 0 \quad (16)$$

$$Q_{x_1} - Q_{x_2} - Q_{x_3} = 0 \quad (17)$$

at x = l + a

$$M_{xx_4} - M_{xx_2} - M_{xx_3} - N_{xx_2} \frac{h}{2} + N_{xx_3} \frac{H}{2} = 0 \quad (18)$$

$$N_{xx_4} - N_{xx_2} - N_{xx_3} = 0 \quad (19)$$

$$N_{xy_4} - N_{xy_2} - N_{xy_3} = 0 \quad (20)$$

$$Q_{x_4} - Q_{x_2} - Q_{x_3} = 0 \quad (21)$$

where M_{ij} are the small additional moment resultants and Q_x is the small additional shear force resultant, needed to move from the primary (membrane) state to the buckled (bent) one.

II.2 Pressure Case

In the case of pressure, the circular cylindrical shells and panels with longitudinal delamination over the entire length are considered. The geometry, loading and coordinate systems are shown on Fig. 1b. The straight edges of the panel are either clamped or simply supported. The location and size of the delamination is arbitrary. Angle α denotes the region of the delamination, while β and γ denote the location of it from left edge and right edge, respectively.

The panel is separated into four parts (four panels) by the delamination. Each part has a set of coordinates attached to it (see Fig. 1b), and the natural plane of the panel lies on the xy-plane. The panel is subjected to uniform external pressure, q, over the entire outer surface. Let h^i (i = I, II, III, IV) denote the thickness of the ith panel (see Fig. 1b). The nondimensional parameter $\bar{h} = h^I/h^{III}$ is used to describe the thickness of the delamination. Let u^i, v^i, w^i (i = I, II, III, IV) be the displacement components of material points on the midplane of each part (each panel) in the x, y, and z directions, respectively. Note that the sign conventions for the two models are different (see Figs. 1a and 1b).

The panel becomes a complete cylindrical shell when the total angle $\phi(\phi = \alpha + \beta + \gamma)$ equals 2π.

The Koiter-Budiansky [14] buckling equations have been deduced from those given in the Appendix of Ref. 14. The version given below corresponds to a set obtained from Sanders-type of kinematic relations [15]. This version, in terms of the small additional displacement components, u, v, and w, is:

$$A_{11}u_{,xx} + 2A_{13}u_{,xy} + A_{33}u_{,yy} + (A_{12} + A_{33})v_{,xy} + A_{13}v_{,xx} + A_{23}v_{,yy} + A_{12}\frac{w_{,x}}{R} + \frac{A_{23}}{R}w_{,y} + q^x = 0$$

$$A_{13}u_{,xx} + (A_{33} + A_{12})u_{,xy} + A_{23}u_{,yy} + (A_{33} + \frac{D_{33}}{R^2})v_{,xx} + (2A_{23} + \frac{2D_{23}}{R^2})v_{,xy} + (A_{22} + \frac{D_{22}}{R^2})v_{,yy} - \frac{qv}{R} + \frac{A_{23}}{R}w_{,x} + (\frac{A_{22}}{R} + q)w_{,y} - \frac{1}{R}[D_{13}w_{,xxx} + (D_{12} + 2D_{33})w_{,xxy} + 3D_{23}w_{,xyy} + D_{22}w_{,yyy}] + q^y = 0$$

$$-\frac{A_{12}}{R}u_{,x} - \frac{A_{23}}{R}u_{,y} - \frac{A_{23}}{R}v_{,x} - \frac{1}{R}(A_{22} + qR)v_{,y} + [\frac{D_{13}}{R}v_{,xxx} + (\frac{D_{12}}{R} + \frac{2D_{33}}{R})v_{,xxy} + \frac{3D_{23}}{R}v_{,xyy} + \frac{D_{22}}{R}v_{,yyy}] - \frac{A_{22}}{R^2}w - [D_{11}w_{,xxxx} + 4D_{13}w_{,xxxy} + (2D_{12} + 4D_{33})w_{,xxyy} + 4D_{23}w_{,xyyy} + D_{22}w_{,yyyy}] + qRw_{,yy} + q^z = 0 \qquad (22)$$

where A_{ij}, D_{ij} (i,j = 1,2,3) are extensional and flexural stiffnesses, q^x, q^y and q^z are corrections to surface loading due to load behavior during buckling, and q is the applied pressure.

The various boundary and auxiliary conditions, associated with y = constant positions, are listed below:

Boundary conditions at $\theta = 0$

(a) Clamped		(b) Simply Supported	
$w^{III} = 0$		$w^{III} = 0$	
$\phi_y^{III} = 0$	(a)	$M_{yy}^{III} = 0$	(b) (23)
$v^{III} = 0$		$N_{yy}^{III} = 0$	
$u^{III} = 0$		$u^{III} = 0$	

Auxiliary Condition at $\theta_3 = \beta$ ($\theta_1 = \theta_2 = 0$)

$$w^I = w^{II} = w^{III}$$
$$\phi_y^I = \phi_y^{II} = \phi_y^{III}$$
$$v^I - (v^{III} + \phi_y^{III} h^{II}/2) = 0$$
$$v^{II} - (v^{III} - \phi_y^{III} h^I/2) = 0$$
$$u^I - (u^{III} + \phi_x^{III} h^{II}/2) = 0$$
$$u^{II} - (u^{III} - \phi_x^{III} h^I/2) = 0$$
$$N_{yy}^I + N_{yy}^{II} - N_{yy}^{III} = 0 \qquad (24)$$
$$N_{xy}^I + N_{xy}^{II} - N_{xy}^{III} = 0$$
$$M_{yy}^I + N_{yy}^I h^{II}/2 + M_{yy}^{II} - N_{yy}^{II} h^I/2 - M_{yy}^{III} = 0$$
$$Q_{y(eff)}^I + N_{xy,x}^I h^{II}/2 + Q_{y(eff)}^{II} - N_{xy,x}^{II} h^I/2 - Q_{y(eff)}^{III} = 0$$

where $Q_{y(eff)} = M_{yy,y} + 2M_{xy,x}$

Auxiliary Conditions at $\theta_4 = 0(\theta_1 = \theta_2 = \alpha)$

$$
\begin{aligned}
&w^I = w^{II} = w^{III}\\
&\phi_y^I = \phi_y^{II} = \phi_y^{III}\\
&v^{II} - (v^{IV} + \phi_y^{IV} h^{II}/2) = 0\\
&v^{II} - (v^{IV} - \phi_y^{IV} h^I/2) = 0\\
&u^I - (u^{IV} + \phi_x^{IV} h^{II}/2) = 0\\
&u^{II} - (u^{IV} - \phi_x^{IV} h^I/2) = 0\\
&N_{yy}^I + N_{yy}^{II} - N_{yy}^{IV} = 0\\
&N_{xy}^I + N_{xy}^{II} - N_{xy}^{IV} = 0\\
&M_{yy}^I + N_{yy}^I h^{II}/2 + M_{yy}^{II} - N_{yy}^{II} h^I/2 - M_{yy}^{IV} = 0\\
&Q_{y(eff)}^I + N_{xy,x}^I h^{II}/2 + Q_{y(eff)}^{II}\\
&- N_{xy,x}^{II} h^I/2 - Q_{y(eff)}^{IV} = 0
\end{aligned}
\qquad (25)
$$

Boundary Conditions at $\phi_4 = \gamma$

(a) Clamped		(b) Simply Supported	
$w^{IV} = 0$		$w^{IV} = 0$	
$\phi_y^{IV} = 0$	(a)	$M_{yy}^{IV} = 0$	(b)
$v^{IV} = 0$		$N_{yy}^{IV} = 0$	(26)
$u^{IV} = 0$		$u^{IV} = 0$	

Note that the simply supported conditions, Eqs. (23b) and (26b) correspond to the classical simply supported conditions, SS-3 [13].

III. Solution Procedure

Axial Compression Case

Elimination of u_i and v_i through the use of Eqs. (2) and (3) and through substitution into Eq. (1) yields a single higher-order ordinary differential equation in w_i alone. Thus, the buckling equation for each region, i, becomes

$$
\begin{aligned}
&[\{A_{xx_i} A_{ss_i} \partial^4/\partial x^4 - (A_{xy}^2 + 2A_{xy}A_{ss} - A_{xx}A_{yy})_i \partial^4/\partial x^2 \partial y^2\\
&+ A_{yy_i} A_{ss_i} \partial^4/\partial y^4\}\{D_{xx_i} \partial^4/\partial x^4\\
&+ 2(D_{xy} + 2D_{ss})_i \partial^4/\partial x^2 \partial y^2 + D_{yy_i} \partial^4/\partial y^4 + N_{xx_i} \partial^2/\partial x^2\}\\
&+ A_{ss_i} A_{xx_i} \{A_{yy} - A_{xy}^2/A_{xx}\}_i \partial^4/\partial x^4] w_i/R^2 = 0
\end{aligned}
$$

$$i = 1,2,3,4 \qquad (27)$$

The solution of the buckling equations can be written as in [13]:

$$
w_i = \sum_{j=1}^{8} A_{ij} \left(e^{\lambda_{ij} \frac{x}{R} \left(\frac{2E_{11}}{\sigma_{cl}}\right)_i^{1/2}}\right) X
$$

$$
\sin S_i \frac{y}{R} \left(\frac{2E_{11}}{\sigma_{cl}}\right)_i^{1/2} \qquad (28)
$$

where

$$
\sigma_{cl_i} = \frac{E_{11}}{3(1 - \nu_{12}\nu_{21})} \frac{t_i}{R}
$$

λ_{ij} are the characteristic roots of the buckling equation, (Eq. (27).

The solution to the buckling equation requires knowledge of 32 constant (A_{ij}, i=1,2,3,4, j=1,2,3,...8). There exist 32 boundary and auxiliary conditions, which are homogeneous in u_i, v_i and w_i and their gradients. These consist of eight boundary conditions, four at each end, Eqs (4) or Eqs. (5), sixteen kinematic continuity conditions, Eqs. (6)-(13), and eight balance conditions in moments and forces, Eqs. (14)-(21).

The use of the above system of boundary and auxiliary conditions yields a system of linear, homogeneous, algebraic equations in A_{ij}. For a nontrivial solution to exist, the determinant of the coefficients must vanish. The determinant contains geometric parameters (L,R,a,h), material parameters (E_{11}, E_{22}, G_{12}, ν_{12}), the applied load, $\bar{p}$, and the circumferential wave number, n.

For a given geometry and material properties, the circumferential wave number (n) is varied and the corresponding load which makes the determinant vanish is obtained. The lowest of these loads is the critical load.

III.2 Pressure Case

For each part, a separated solution is assumed, which satisfies the classical simply supported boundary conditions at x = 0 and L. This is done for the special construction for which there is no coupling between extension and bending, extension and shear, and between bending and twisting action. This means that for all parts

$$B_{ij} = A_{13} = A_{23} = D_{13} = D_{23} = 0 \qquad (29)$$

The classical simply supported boundary conditions are denoted by

$$SS3: \quad w = M_{xx} = N_{xx} = v = 0 \qquad (30)$$

The separated solution is characterized by

$$
\begin{aligned}
u(x,y) &= U(y) \cos \frac{m\pi x}{L}\\
u(x,y) &= V(y) \sin \frac{m\pi x}{L}\\
w(x,y) &= W(y) \sin \frac{m\pi x}{L}
\end{aligned}
\qquad (31)
$$

Substitution of Eqs. (31) into Eqs. (22) for the special construction, Eqs. (29), yields

$$L_{11}U + L_{12}V + L_{13}W = 0$$
$$L_{21}U + L_{22}V + L_{23}W = 0 \qquad (32)$$
$$L_{31}U + L_{32}V + V_{33}W = 0$$

where the L_{ij} are linear differential operators.

Elimination of U and V through the use of the first two of Eqs. (32) and substitution into the third one yield a single higher order ordinary differential equation in W alone. This higher order equation assumes the form

$$F_8 \frac{d^8w}{d\theta^8} + F_6 \frac{d^6w}{d\theta^6} + F_4 \frac{d^4w}{d\theta^4} + F_2 \frac{d^2w}{d\theta^2} + F_0 = 0 \qquad (33)$$

where the F's are constants that contain the external load q and structural geometric parameters (A_{ij}, D_{ij}, $\bar{h}$, R, etc.). Note that some of the F's change according to the case of load behavior during buckling.

The solution procedure is similar to the one described for rings and arches in Article 7.3 of Ref. 16. The number of equations is greater, the equations themselves are more complex, and a closed form solution is not expected as in Ref. 16. Nevertheless, the overall procedure can be followed and a numerical estimate can be achieved. Thus, first assume for $W(\theta)$ a solution of the form

$$W = C\exp(r\theta) \qquad (34)$$

Since the order of the equation is eight, then substitution into Eq. (33) yields an eighth degree polynomial in r. Thus, eight roots are expected for each geometry and load level. If the eight roots are distinctly different, the general solution for $W(\theta)$ is given by

$$W(\theta) = \sum_{i=1}^{8} C_i \exp(r_i\theta) \qquad (35)$$

If double roots occur, the form of Eq. (34) is modified accordingly.

The form of the solution for $U(\theta)$ and $V(\theta)$ is similar to that of Eq. (35) and the solution for U, V and W is given in terms of eight constants.

There exist eight unknowns, C_i's, for each part, and the total number of unknowns is 32. Use of the 32 boundary and auxiliary conditions leads to a system of 32 linear, homogeneous algebraic equations in 32 unknowns. For a nontrivial solution to exist the determinant of the coefficients must vanish. This yields the characteristic equation.

IV Applications

IV.1 Axial Compression Case

Results are generated for a cylindrical shell made up of isotropic laminae and for both simply supported and clamped boundary conditions. Since for each type of supports (simple and clamped supports) there are four types of boundary conditions, results are generated for the weakest and for the strongest configurations, which are known as SS1 ($w = w_{,xx} = \sigma_{xx} = \tau_{xy} = 0$) and CC4 ($w = w_{,x} = u = v = 0$), respectively. The boundary conditions are assumed to be the same at both ends, i.e. both ends are SS1 or CC4. The dimensions of the cylindrical shell are such that L/R=5, and R/t=30, where L, R and t are the length, radius and thickness of the shell, respectively.

Figure 2 shows the effect of delamination length and through-the-thickness position on the critical loads of a simply supported cylindrical shell (SS1). The delamination is assumed to be located symmetrically with respect to both ends of the shell. The critical loads are normalized with respect to the critical load of the classical theory. The figure shows that for a delamination in the middle surface of the cylindrical shell, the delamination has a negligible effect on the critical loads as long as the delamination is far from the edges (effect of position with respect to the edges will be discussed in another figure). As the delamination moves away from the middle surface of the shell, its presence becomes important. For a delamination thickness $\bar{h} = 0.3$, the delamination has no effect on the critical loads, as long as the delamination length is small ($\bar{a} < .04$). As the delamination length increases the critical load decreases and it approaches asymptotically a value, which is, approximately 60% of the critical load of the perfect configuration. As the delamination moves closer and closer to the other surface, a sharp drop in

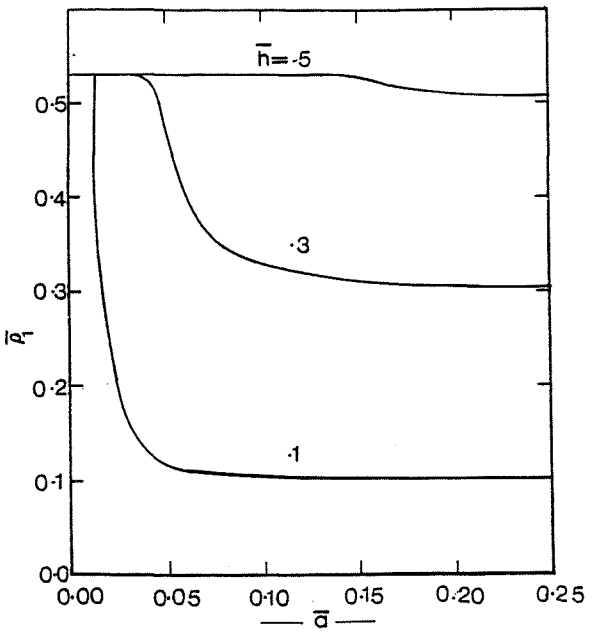

Fig. 2. Effect of Delamination Length on the Critical Loads (Complete Cylinder; SS1)

the critical load is noticed at a very small delamination length ($\bar{a}$ = 0.01). This drop in the critical load continues till it reaches a constant value (20% of that of the perfect shell), at a value for the delamination length parameter of $\bar{a}$ = 0.1.

A similar set of curves is obtained for clamped boundary conditions. The effect of delamination length on the critical loads of a symmetrically delaminated cylindrical shell, for different values of the delamination thickness, is shown in Fig. 3. This figure, illustrates that, only for very small values for the delamination length ($\bar{a}$ < .01), the delamination has no significant effect on the critical loads, regardless of the value for $\bar{h}$. For larger values for the delamination length parameter, $\bar{a}$, a noticeable drop in the critical loads is observed.

The effect of lengthwise delamination position on the critical loads is also studied. Figure 4 presents results for $\bar{a}$ = 0.1. For delamination thickness $\bar{h}$ < 0.3, the delamination position, $\bar{l}$, has no appreciable effect on the critical loads. For larger values of $\bar{h}$, $\bar{h}$ > 0.3, the position of delamination has an important effect on the critical load, and this effect increases as $\bar{h}$ increases. For instance, a reduction of about one third in the critical load is noticed for a delamination near the edge (by comparison to the critical load of a delamination far from the edge; $\bar{l}$> .08), for a midsurface delamination, $\bar{h}$ = 0.5. The position effect decreases as the value of $\bar{h}$ decreases.

Unlike the simply supported case, the position of delamination w.r.t. the edges of the shell with clamped ends, has virtually no effect on the critical loads, for delamination length $\bar{a}$ = 0.1, regardless of the value of $\bar{h}$, as shown on Fig. 5.

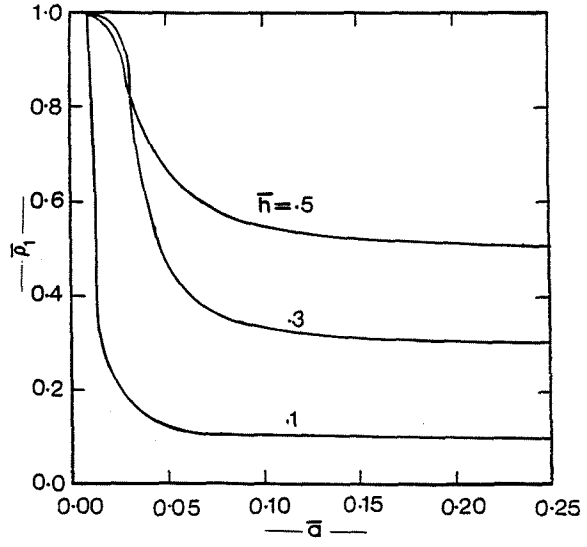

Fig. 3. Effect of Delamination Length on the Critical Loads (Complete Cylinder; CC4)

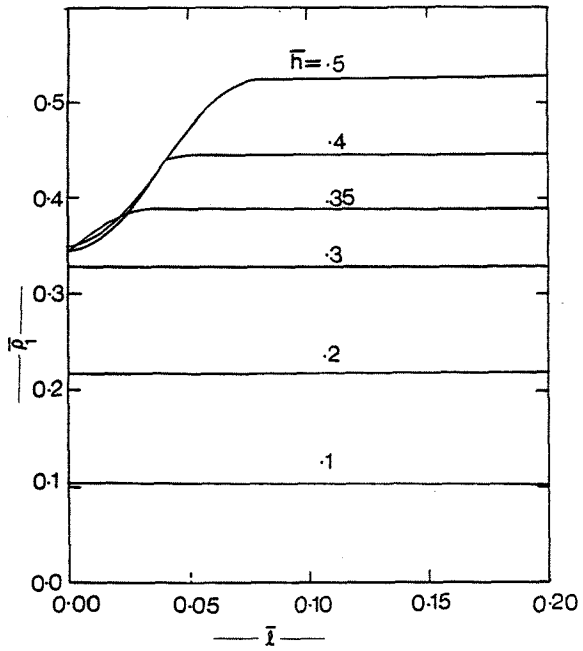

Fig. 4. Effect of Delamination Position on the Critical Loads (Complete Cylinder; SS1)

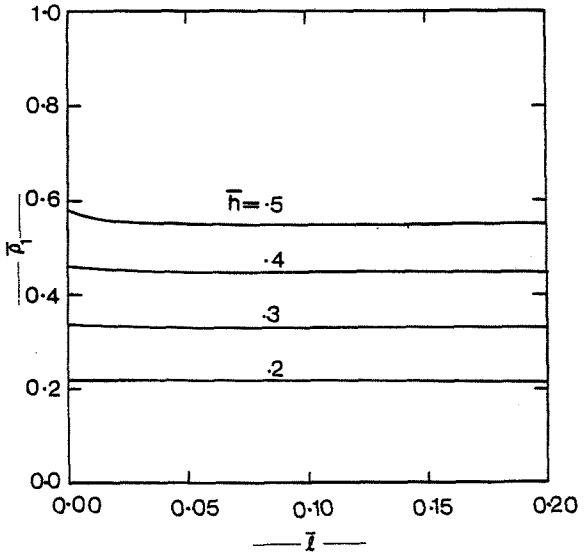

Fig. 5. Effect of Delamination Position on the Critical Loads (Complete Cylinder; CC4)

IV.2 Pressure Case

Critical loads for complete thin laminated cylindrical shells and thin laminated cylindrical panels, with delamination of constant width and extending over the entire length, are calculated. The material used is graphite/epoxy and the orthotropic axes of each ply are at 0° and 90° with the structural axes.

The engineering constants, typical of this material, are

$$E_L/E_T = 40;\ G_{LT}/E_T = 0.5,\ \nu_{LT} = 0.25 \qquad (16)$$

where E_L is the tensile modulus in the filament direction (20.685×10^{10} N/m^2; 30×10^6 psi),

E_T is the modulus in the transverse direction (0.517×10^{10}N/m^2; 0.75×10^6 psi),

G_{LT} is the shear modulus (0.759×10^{10} N/m^2; 0.375×10^6 psi), and

ν_{LT} is Poisson's ratio.

The generated results are used to assess the effect of various parameters on the critical load for symmetric cross-ply delaminated shells primarily with stacking sequence $[90°/0°/90°]_{10T}$. Note that each part is a regular symmetric cross-ply laminate, repeated ten times.

Fig. 6 shows the effect of "through-the-thickness" delamination position, $\bar{h}$, and of delamination (size) width α on the critical load parameter, $|\lambda|(\lambda = qR^3/D_{11}^{III})$.

It is seen that for small values of α (delamination size) the presence of delamination has a small effect on the critical load regardless of $\bar{h}$- values. As the delamination size or width increases the reduction in the value of the critical load is very pronounced, especially as the position of delamination ($\bar{h}$) moves closer to the free surfaces of the laminate ($\bar{h}$ = 0.3 or 0.7 and 0.1 or 0.9). Note that because the employed analysis is a linear bifurcation analysis the critical loads corresponding to $\bar{h}$ and $(1-\bar{h})$ are identical. It is expected that the postbuckling behavior of shells with $\bar{h}$ will be very different from that of shells with $(1-\bar{h})$.

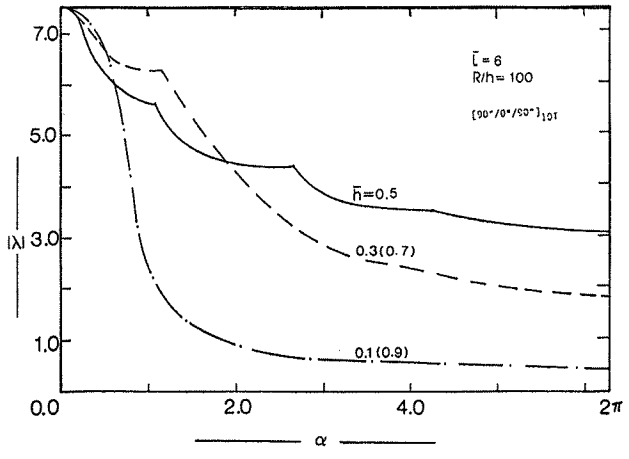

Fig. 6. Critical Pressures for Symmetric, Cross-Ply, Delaminated Cylinders

The effect of delamination width (size) α for various length to radius values, $\bar{L}$, is shown on Figs. 7 and 8, for a panel of $\phi = \pi/2$, with clamped and simply-supported edge boundaries, respectively. These results correspond to R/h = 100 and to midsurface delamination, $\bar{h}$ = 0.5, but they are typical of almost all other configurations corresponding to different R/h and $\bar{h}$ values.

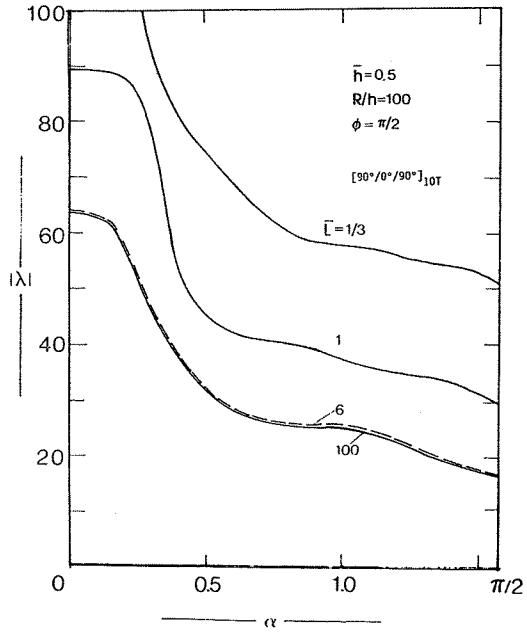

Fig. 7. Effect of Delamination Width on the Critical Pressure (Clamped Panel; $\phi = \frac{\pi}{2}$)

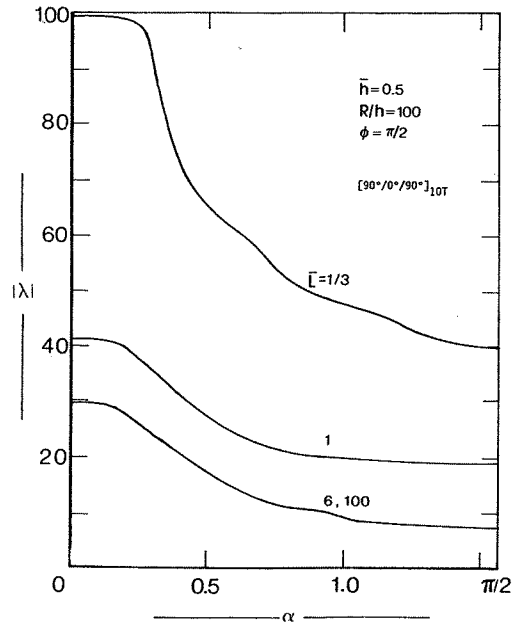

Fig. 8. Effect of Delamination Width on the Critical Pressure (Simply Supported Panel; $\phi = \frac{\pi}{2}$)

It is seen from Figs. 7 and 8 that the critical load parameter decreases with increasing delamination width α, and with increasing $\bar{L}$ values. A comparison between the results of Figs. 7 and 8 shows that clamping the straight edges has a stabilizing effect. This effect is influenced by both $\bar{L}$ and α. Note that for $\bar{L}$ = 1/3 the initial load is increased by approximately 25% for $\alpha = \pi/2$. This increase changes as α decreases and it becomes approximately 44% when α = 0. Similar trends are observed for other $\bar{L}$- values but the percentages become higher with increasing $\bar{L}$-value.

Moreover, the effect of delamination position from the edge of the panel, β, on the critical load parameter is shown on Tables 1 and 2. The results correspond to an isotropic laminate of $\phi = \pi/2$ with clamped and simply supported boundaries, respectively, and for a delamination size, α, of 0.2 radians. Results are presented for various positions, β, and several through-the-thickness positions, $\bar{h}$. It is seen that this effect is relatively small for $\bar{h}$ = 0.5 and 0.3 (0.7), but negligibly small for $\bar{h}$ = 0.1(0.9) and 0.01 (0.99).

Table 1. Effect of Delamination Location on Critical Pressure (Clamped Panel; $\phi = \frac{\pi}{2}; \alpha = 0.2$)

β \ $\bar{h}$	0.5	0.3	0.1	0.01
0.0	28.8847	29.6901	20.1663	0.2018
0.1	29.2059	30.6522	20.1665	0.2018
0.2	28.9962	30.2359	20.1668	0.2018
0.3	28.4068	28.6646	20.1673	0.2018
0.4	28.0669	27.8684	20.1673	0.2018
0.5	28.3650	28.5085	20.1668	0.2018
0.6	28.9675	29.9942	20.1665	0.2018
0.6854	29.2115	30.7097	20.1663	0.2018

Table 2. Effect of Delamination Location on the Critical Pressure (Simply Supported Panel; $\phi = \pi/2; \alpha = 0.2$)

β \ $\bar{h}$	0.5	0.3	0.1	0.01
0.0	8.2869	10.7108	2.2364	0.0224
0.1	8.0421	9.6941	2.2366	0.0224
0.2	7.7323	8.9581	2.2366	0.0224
0.3	7.5215	8.6057	2.2366	0.0224
0.4	7.4127	8.5228	2.2366	0.0224
0.4854	7.3854	9.4696	2.2368	0.0224

V. Discussion and Recommendations

A linear bifurcation analysis was performed and critical loads were derived for laminated complete cylindrical shells and panels of isotropic or special cross-ply construction under axial compression and uniform pressure, respectively.

An important observation is that for very small values of the delamination width the presence of delamination does not appreciably alter the perfect (free of delaminations) geometry critical load. In this case it is safe to say that the critical load, adjusted by some reasonable knockdown factor to account for the presence of initial geometric imperfections, is a good measure of the load carrying capacity of the system. On the other hand, for large delamination widths, especially as the position of delamination moves closer to the free surfaces of the laminate, the critical load is very small. In this case, one should not relate the critical load to the load carrying capacity of the system. Instead, failure will be governed by delamination growth, which of course depends on the fracture toughness of the material. This point has been addressed extensively in [8-10].

It is observed that the most influencing parameters for a given laminated geometry is the size of the delamination, and its through the thickness position for both load cases.

Another observation is that for the pressure case, the effect of boundary conditions (along the straight edges) has an important effect (see Figs. 7 and 8). On the other hand, for axial compression the effect of boundary conditions (ends) is insignificant for large delaminations (see Figs. 2 and 3).

It is also observed that the effect of delamination position from the edge of the panel, under pressure, is insignificant. For the axial compression case, the effect of the delamination position along the length of the cylinder (effect of l_1; see Fig. 1a) for clamped boundaries is also negligible, while for simply-supported ends it is small but not negligible.

The results obtained for the two load cases seem to be reasonable. However, there exist two points that need special attention. One is that in some cases the buckling mode of the two parts that are separated by the delamination (parts 2 and 3 in Fig. 1a, parts I and II in Fig. 1b), suggests contact over a certain portion. The second one is that, for the pressure case, the values of the pressure load acting upon the two parts (part I and II; see Fig. 1b) may take a finite jump during the buckling process, i.e., in the prebuckling state, the loads upon two parts are $\bar{h}q$ and $(1 - \bar{h})q$, respectively, while in the fully developed postbuckling state they become q and 0, respectively. The above two points are not taken into account in the present model for buckling analysis, which may have some influence upon the accuracy of the solution.

Needless to say that further and more detailed studies need be performed before we acquire complete and full understanding of delamination buckling and growth of laminated shells. It is necessary to derive a new mathematical model which will account for the contact between delaminated layers and finite change of loads, during buckling. Moreover, the model must be applicable to postbuckling behavior. This is needed for performing delamination growth studies.

References

1. Whitcomb, J. D., "Finite Element Analysis of Instability Related Delamination Growth," J. Composite Materials, Vol. 15, 1981, pp. 403-426.

2. Shivakumar, K. N. and Whitcomb, J. D., "Buckling of a Sublaminate in a Quasi-Isotropic Composite Laminate," J. Composite Materials, Vol. 19, 1985, pp. 2-18.

3. Yin, W. L. and Wang, J. T. S., "Postbuckling Growth of a One-Dimensional Delamination. Part I - Evaluation of the Energy Release Rate," J. Appl. Mechanics, Vol. 51, No. 4, 1984, pp. 939-941.

4. Yin, W. L. and Fel, Z. Z., "Buckling Load of a Circular Plate with a Concentric Delamination," Mechanics Research Communications, Vol. 11, No. 5, 1984, pp. 337-344.

5. Gillespie, Jr., J. W. and Pipes, R. B., "Compressive Strength of Composite Laminates with Interlaminar Defects," Composite Structures, Vol. 2, 1984, pp. 49-69.

6. Wang, S. S., "Edge Delamination in Angle-Ply Composite Laminates," AIAA Journal, Vol. 22, No. 2, 1984, pp. 256-264.

7. Chai, Herzl and Babcock, C. D., "Two-Dimensional Modelling of Compressive Failure in Delaminated Laminates," J. Composite Materials, v. 19, 1985, pp. 67-98.

8. Simitses, G. J., Sallam, S. and Yin, W. L., "Effect of Delamination of Axially Loaded Homogeneous Laminated Plates," AIAA Journal, Vol. 23, No. 9, 1985, pp. 1437-1444.

9. Simitses, G. J. and Sallam, S., "Delamination Buckling and Growth of Flat Composite Structural Elements," AFOSR-TR-84-xxxx (written under Grant AFOSR 83-0243) Ga. Tech, Atlanta, Ga., 1984.

10. Yin, W. L., Sallam, S. N. and Simitses, G. J., "Ultimate Axial Load Capacity of a Delaminated Beam-Plate," AIAA Journal, Vol. 24, No. 1, 1986, pp. 123-128.

11. Troshin, V. P., "Effect of Longitudinal Delamination in a Laminar Cylindrical Shell on the Critical External Pressure," Mechanics of Composite Materials, Vol. 17, No. 5, 1983, pp. 563-567.

12. Troshin, V. P., "Use of Three-Dimensional Model of Filler in Stability Problems for Triple-Layer Shells with Delaminations," Mekhanika Kompozitnykh Materialov, No. 4, 1983, pp. 657-662.

13. Hoff, N. J., "The Perplexing Behavior of Thin Circular Cylindrical Shells in Axial Compression: Israel Journal of Techn., Vol. 4, No. 1, 1966, pp. 1-28.

14. Budiansky, B., "Notes on Nonlinear Shell Theory," Journal of Applied Mechanics, Vol. 35, No. 2, June 1968, pp. 393-401.

15. Sanders, J. L., "Nonlinear Theories of Thin Shells," Quarterly of Applied Mathematics, Vol. 21, 1963, pp. 21-36.

16. Simitses, G. J., Elastic Stability of Structures, Prentice-Hall, Inc., Englewood Cliffs, N.J., 1976 (second printing R. E. Krieger Publishing Co., Melbourne, FL, 1985).